Distribution of chains in polymer brushes produced by a "growing from" mechanism

Andre Martinez,[†] Jan-Michael Y. Carrillo,[‡] Andrey V. Dobrynin,[§,*] and Douglas H. Adamson[†,*]

[†]Department of Chemistry and Polymer Program, Institute of Materials Science, University of Connecticut, Storrs, CT 06250

[‡]National Center for Computational Science, Oak Ridge National laboratory, Oak Ridge, TN 37831

[§]Department of Polymer Science, University of Akron, Akron, OH 44325-3909

Abstract: The molecular weight and polydispersity of the chains in a polymer brush are critical parameters determining the brush properties. However, the characterization of polymer brushes is hindered by the vanishingly small mass of polymer present in brush layers. In this study, in order to obtain sufficient quantities of polymer for analysis, polymer brushes were grown from high surface area fibrous nylon membranes by ATRP. The brushes were synthesized with varying surface initiator densities, polymerization times, and amounts of sacrificial initiator, then cleaved from the substrate and analyzed by GPC and NMR. Characterization showed that the surface-grown polymer chains were more polydisperse and had lower average molecular weight compared to solution-grown polymers synthesized concurrently. Furthermore, the molecular weight distribution of the polymer brushes was observed to be bimodal, with a low molecular weight population of chains representing a significant mass fraction of the polymer chains at high surface initiator densities. The origin of this low MW polymer fraction is proposed to be the termination of growing chains by recombination during the early stages of polymerization, a mechanism confirmed by molecular dynamics simulations of brush polymerization.

INTRODUCTION

Polymer brushes are of interest for a range of applications that include non-biofouling,[1,2] cell adhesion,[3,4] low friction surfaces,[5,6] organic electronics,[7,8] tunable colloidal systems,[9,10] and stimuli-responsive materials.[11,12] Stretching of the polymer chains as a result of their close packing in a brush is the basis for their unique properties and is known to be affected by both the molecular weight (MW) and polydispersity index (PDI) of the brush chains.[13,14] Despite their considerable interest, however, the direct characterization of polymer brushes can be problematic, largely due to the vanishingly small mass of polymer that constitute a typical brush. In this study we use a high surface area nylon filters composed of fibers, which, on the scale of the polymer brush, are effectively flat surfaces. Cleaving the polymer chains from the surface provides sufficient material to directly characterize the polymer brushes by GPC and NMR.

Polymer brushes are synthesized by several polymerization mechanisms, including: ionic,[15,16] ring-opening,[17] radical,[18] and controlled radical polymerizations, most notably atom transfer radical polymerization (ATRP),[12,19] with two general strategies to prepare the brush. In one approach, grafting-to, pre-made polymers are attached to a surface. This approach benefits from the ability to easily characterize the polymers constituting the brush, as their MW and PDI can be measured prior to surface attachment, but it suffers from limited brush densities as the first polymer chains attached shield the surface from the attachment of additional chains.

In a second approach, grafting-from, the polymers are grown from initiation sites attached to the substrate. The grafting-from approach, used in our investigation, is more common and has the advantage of being able to form denser brushes, but characterization of the MW and PDI of these brushes is difficult. To overcome the difficulty in characterizing growing-from brushes, it is common to use polymers concurrently grown in solution as a "stand-in" for the brush polymer in MW and PDI analysis.[12] These solution polymers are grown by using a "sacrificial initiator", where initiator is added to the solution in which the brush is grown. The MW and PDI of the polymers in the brush are then inferred from the solution grown polymers rather than characterizing the polymer brush directly. This approach was first reported by Marutani *et al.* who used ATRP to grow poly(methyl methacrylate) (PMMA) from magnetite nanoparticles.[20] In that work, polymers were cleaved from high surface curvature particles and compared to polymers grown in a solution, and it was observed that the MW and PDI of the two polymers were nearly identical.

However, the sacrificial initiator technique for describing the MW and PDI of brush polymers is still contentious, as substrate geometry has been shown to play a significant role. Genzer *et al*. studied PMMA grown by ATRP from substrates including porous silicon (pore size~50 nm), anodically etched aluminum oxide (pore size~200 nm), and in solution.[21] They found, using mass spectroscopy, that MW was lowest for the porous silicon grown polymer and highest for the solution grown polymer. They attributed this finding to the progressive confinement of polymer chains in a concave environment. Using ellipsometry, Kim *et al*. found that, unlike solution grown polymers, the rate of brush thickness growth

slowed over time. They attributed this to the higher concentration of radicals found in a growing brush resulting in a higher rate of termination than is found in solution grown polymers.[22] A recent report by Patil *et al.* focused on the use of tetrabutylammonium fluoride to cleave PMMS chains from a silica surface and found that a higher $Cu^{(II)}/Cu^{(I)}$ ratio led to an increase in the apparent grafting density. Due to experimental uncertainties, the authors exercised caution and referred to their measured grafting densities as apparent grafting densities. In addition, the authors speculated on the existence of a low MW population of grafted polymers, but were unable to observe them due to a lack of instrumental sensitivity.[23] Computational studies of polymer brushes grown both with[24] and without[25] sacrificial initiator predict that brush density decreases with distance from the surface due to the stunted growth of shorter chains arising from a monomer concentration gradient as well as from termination. Increasing initiator density in these simulations exacerbates the phenomenon.

In the results reported here, we find significant differences in the MW and PDI between surface grown and solution grown polymer. Further, we observe a bimodal molecular weight distribution (MWD) for the surface-grown polymer brushes, with low MW polymers constituting a considerable fraction of the total polymer mass, especially at higher initiator densities. While this low MW fraction has not been reported previously, the results of several groups have hinted at its presence.[22,26] Huang *et. al*. grew 2-hydroxyethyl methacrylate (HEMA) from gold surfaces by ATRP and reported that the loose packing of grafted chains indicated that only 10% of the surface bound initiator led to high molecular weight polymer. They hypothesized the remainder never initiated or was lost via early termination reactions.[27] Our results provide experimental evidence and computational corroboration that many chains stop growing during the early stages of the surface-initiated polymerization, by termination resulting from the high concentration of active centers. This early termination effectively reduces the grafting density of the polymer brushes.

EXPERIMENTAL SECTION

Materials: 2-bromoisobutyryl bromide (BrIbB)(Acros, 98%), isobutyryl bromide (IbB)(TCI, >95 %), CuBr (Strem Chemicals, 98 %), $CuBr_2$ (Fisher, reagent grade), N,N,N',N'',N''-

pentamethyldiethylenetriamine (PMDETA)(Aldrich, 99+ %), methanol (Aldrich, 99.8 %), tetrahydrofuran (THF)(Fisher, histological grade), sodium hydroxide (Fisher, pellets), formaldehyde (Fisher, 37 wt %, Certified ACS), phosphoric acid (Acros, 85 wt %) and 35 kg/mol poly(methyl methacrylate) (PMMA)(Scientific Polymer Products Incorporated) were used as purchased without further purification. Acetone (Fisher, histological grade) was dried with $CaSO_4$ then distilled and stored over 3 Å molecular sieves and degased. Methyl methacrylate (MMA) (Aldrich, 99 %) was rinsed three times with 5 wt % $NaOH_{(aq)}$, and three times with distilled water, then dried with $CaCl_2$, distilled under reduced pressure, and stored over CaH_2 at -32 $^{\circ}$C. Triethylamine (Acros, 99 %) and chloroform (Fisher, histological grade) were dried with $CaSO_4$, distilled under reduced pressure, and then stored over CaH_2.

Methods: Fourier transform infrared spectroscopy (FTIR) was performed using a Magna-IR 560 spectrometer with an ATR accessory. Samples were prepared by drying in a vacuum oven and were used without further modification. X-ray photoelectron spectroscopy (XPS) was performed using a Phi Multiprobe Model 25−120 instrument. Nylon samples were adhered to a sample holder using carbon tape. Binding energies were used to determine the presence of carbon, oxygen, nitrogen, and bromine atoms. NMR spectra were obtained with a Bruker AVANCE III 400 instrument using $CDCl_3$ as a solvent. Gel permeation chromatography (GPC) was preformed using a Waters 717 plus autosampler with THF as eluent, a Waters 1515 isocratic HPLC pump, a Jordi flash gel DVB column, and a Varian 380-LC ELS detector. For scanning electron microscopy (SEM) analysis, nylon samples were adhered to a SEM stub using carbon tape. Samples were then coated with gold/palladium using a Polaron Instruments SEM coating unit E5100 for approximately 40 s. Images were taken on a JEOL 6335F field emission (FESEM) instrument operating at 12 kV accelerating voltage and a 8-15 mm working distance.

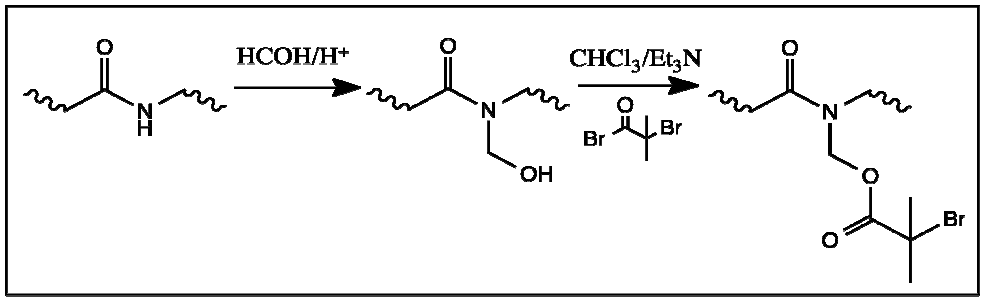

Scheme 1. Reaction for functionalization of nylon membranes using the acid bromide 2-bromoisobutyryl bromide (BrIbB).

Membrane Functionalization: 13 mm diameter Whatman 0.2 µm nylon membrane filters were functionalized for ATRP by techniques previously descsribed.[28] Membranes were first rinsed with acetone and dried with air, then placed in 10 ml of 37 wt % formaldehyde and 0.4 ml of 85 wt % phosphoric acid was added. Membranes were stirred in this solution for approximately two hours at 60-70 °C, then rinsed with distilled water followed by acetone and dried under vacuum. The reaction scheme leading to initiator-functionalized membranes is shown in Scheme 1. Steps of the functionalization were followed by FTIR (Figure 1) and XPS (Figure SI1 of supplementary information). XPS was used to verify attachment of BrIbB due the carbonyl peaks of BrIbB overlapping with nylon carbonyl peaks in FTIR.

Next, membranes were placed in a vial with 10 ml chloroform and 0.8 ml triethylamine and chilled in an ice bath while solutions of BrIbB and IbB were made at various molar ratios from 0-100 % BrIbB. 0.20 ml of these acid bromide solutions were added to the vial in each case and white smoke was formed. The flask was topped with argon or nitrogen before sealing and stirring on an ice bath. The bath was allowed to come to room temperature and the membranes sat in the solution approximately two hours. Next, membranes were rinsed with acetone and distilled water before drying under vacuum.

Polymerization: Polymerizations were prepared inside a nitrogen-filled glovebox. First, CuBr (0.48 mmol, 0.067 g), CuBr2 (0.048 mmol, 0.011 g) and PMDETA (0.51 mmol, 0.11 ml) were dissolved in acetone (5.0 ml). Next, MMA (48 mmol, 5.0 ml) was added immediately followed by initiator functionalized membranes and the contents were stirred at room temperature for an allotted period of time.

The reagents MMA, CuBr, $CuBr_2$, and PMDETA were used in a 100:1.0:0.10:1.1 molar ratio. When sacrificial initiator was used, it was added last via syringe at the start of the polymerization. Polymeriza-

tions were terminated with degased methanol. Membranes were rinsed extensively with acetone. Mild bath sonication was employed to assist in the removal of physically adsorbed solution grown polymer.

Precipitation and Chain Cleavage: Terminated polymerizations were decanted to methanol. Resulting precipitated polymer was redissolved in THF and precipitated into methanol to assist in the removal of copper salts. Polymer chains were cleaved from nylon membranes by stirring overnight in 0.5 M $NaOH_{(aq)}$ at approximately 60 °C, then solutions were decanted into methanol. Polymer was collected by filtration and redissolved/precipitated to remove salts.

RESULTS AND DISSCUSSION

Polymer brushes are grown from nylon filters composed of fibers that are nearly flat on the scale of the brush spacing. The average curvature of the fibers is 4.9×10^{-3} nm^{-1} (see SI1 for calculation), meaning that points on a fiber separated by 1 nm would vary in height by, at most, 0.024 Å. Thus from the point

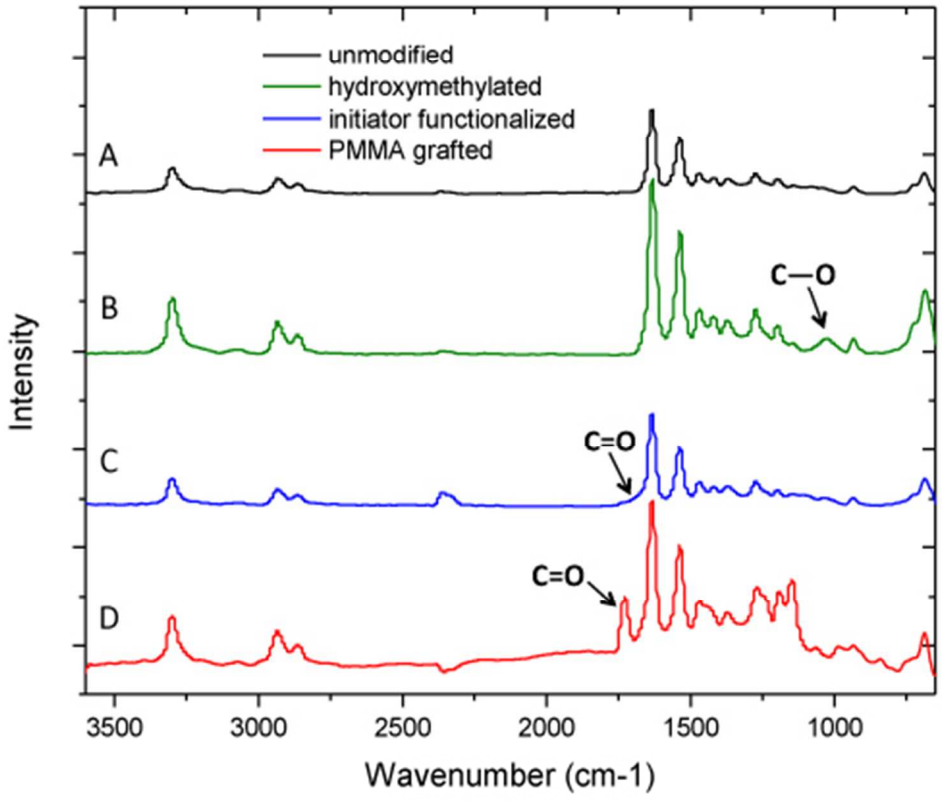

Figure 1. FTIR spectra of membrane surfaces. A) the unmodified membrane shows all peaks expected for nylon. B) Hydroxymethylation introduces a peak at 1030 cm^{-1} corresponding to C—O stretching. C) Functionalization with BrIbB gives the C=O stretching peak at 1700 cm^{-1} that appears as a shoulder to the amide carbonyl stretching peak of the membrane. D) Post polymerization showing a C=O stretch from PMMA observed at 1730 cm^{-1}.

of view of the growing polymer chain, the surface is flat. This is significant, as highly curved convex surfaces, unlike flat surfaces, provide increasing volume for chains to occupy as they grow further from the surface.

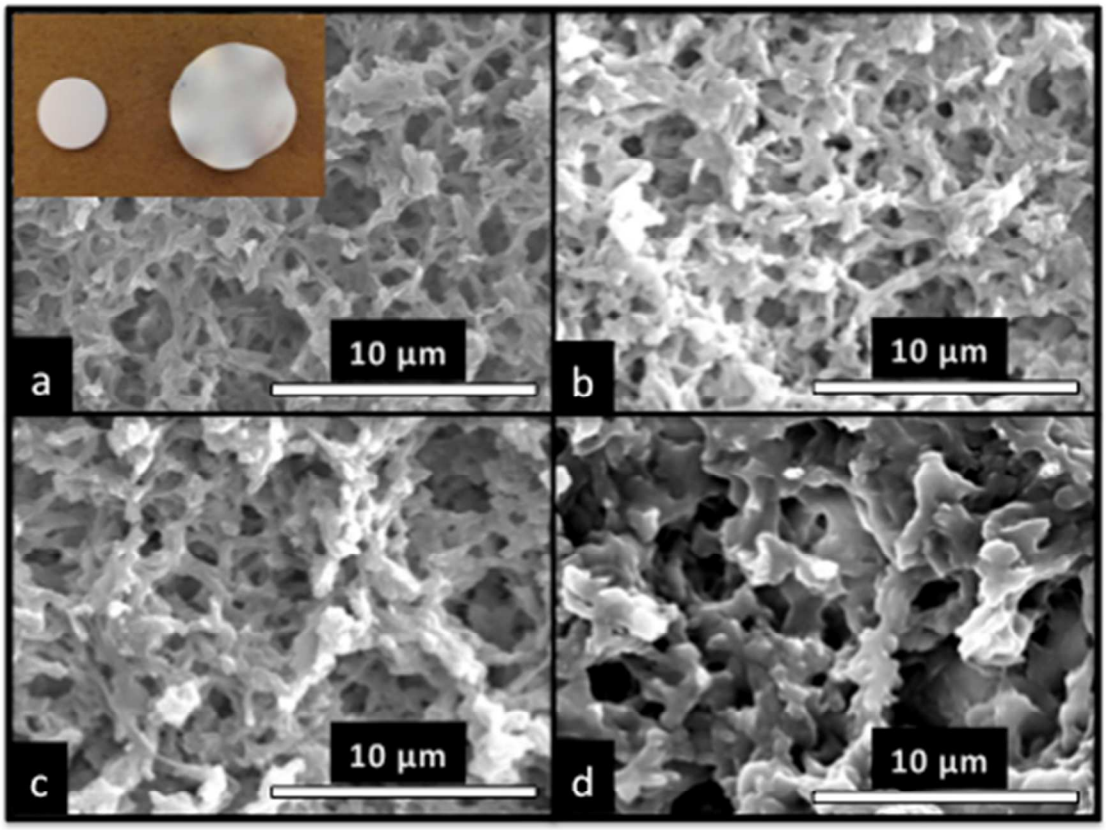

Figure 2. SEM images of (a) membrane prior to polymerization, (b-d) 30%, 50%, 100% mol initiator functionalized membrane respectively post polymerization. The inset image shows a membrane pre (left) and post (right) polymerization.

To grow polymers from the nylon surface, the filters are functionalized with 2-bromoisobutyryl bromide (BrIbB). This acid bromide contains an alkyl bromide and is a well-known ATRP initiator. To vary the density of initiator on the surface, the BrIbB is diluted with isobutyryl bromide (IbB), also an acid bromide, but lacking the necessary alkyl bromide for ATRP initiation. This reaction is outlined in Scheme 1. While the functionalization of the membrane with BrIbB results in an ATRP initiator attached to the membrane, reaction with IbB serves to block the placement of an active ATRP initiator at that position. The functionalization of the surface is followed by FTIR, as shown in Figure 1, as well as being demonstrated by XPS (Figure SI1).

The membranes are prepared with molar ratios of BrIbB to IbB from 1 to 0. Although both molecules react with the membrane surface by way of an acid bromide, their reactivity is not identical, as indicated by a test reaction using cryogenically ground nylon powder in an NMR tube. Comparing the initial concentrations of BrIbB and IbB in the tube before and after the addition of the nylon (shown in

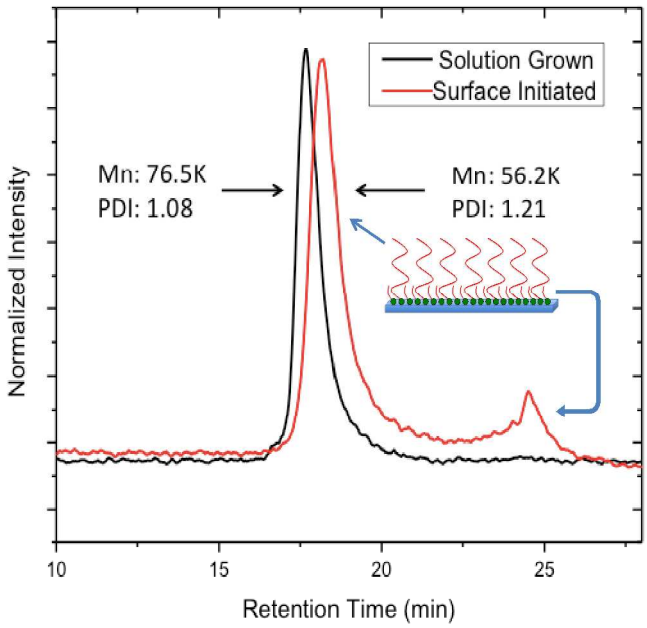

Figure 3. GPC spectra of solution (black) and cleaved surface-initiated (red) PMMA. The inset cartoon illustrated the proposed origins of the two peaks in the surface-initiated polymer spectrum. The solution grown polymer is of higher MW and narrower polydispersity and does not contain the low MW fraction found in the surface grown polymers.

Figure SI2) indicates the BrIbB is approximately 2.5 times more reactive than IbB towards the nylon powder in deuterated chloroform. While this means that the initiator/blocker molar ratio on the surface is greater than the molar ratio used to functionalize the surface, for simplicity the BrIbB/IbB mole fraction used to functionalize the surface is reported to indicate the relative density of surface functionalization. Also, due to the fibrous morphology of our membranes, accurate measurements of grafting densities are difficult, as the use of commonly applied techniques to measure brush height are not accurate with a fiber network. Nonetheless, by using image analysis of numerous SEM images of a 100 % functionalized filter to estimate the increase in fiber thickness due to the growth of brushes from the surface, and comparing that result to the GPC molecular weight of the removed polymer, we find a grafting density of 0.842 chains per nm^2 (see Table S1 in the SI for details). However, as explained in the following sections, the density of attached initiator is likely much higher, as this analysis includes only high MW chains.

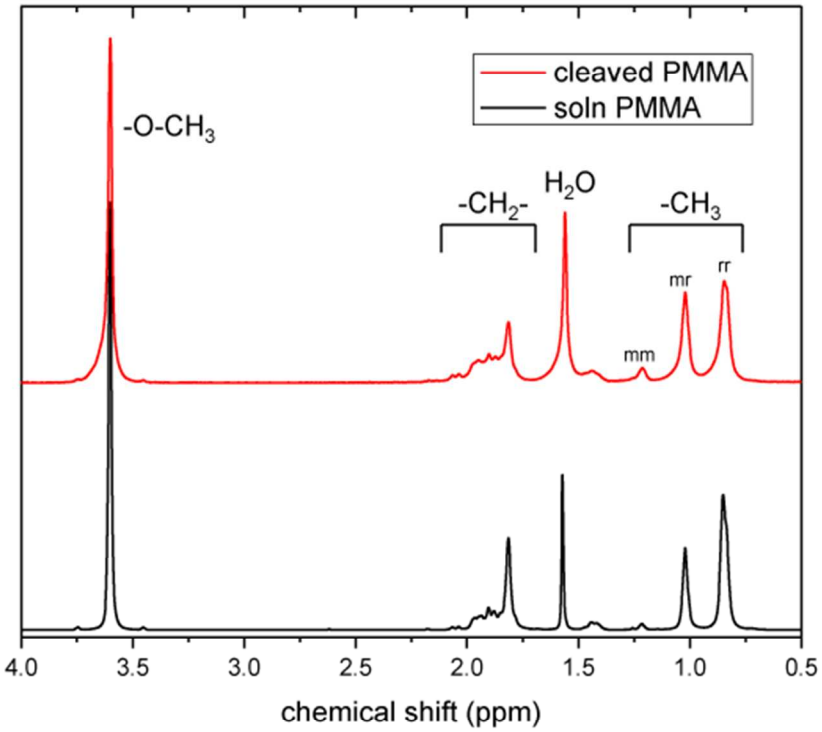

Figure 4. Proton NMR comparison of: top) polymer cleaved from the surface of the filter, and bottom) polymer grown in solution. From these results it is clear the cleaved polymer does not contain any significant degradation products of the nylon surface.

SEM images show that after polymerization, individual fibers in the membrane are thicker with increasing initiator density. Figure 2a is an SEM image of a filter prior to polymerization. Figures 2b through 2d show membranes that have been reacted with monomer for the same amount of time, but differ in the density of initiation. A macroscopic indication of the surface density of initiator is the observation that the more densely functionalized the membrane, the greater its expansion, as shown in the inset of Figure 2a and Figure SI3. Membranes that are reacted with only IbB, and thus not functionalized with initiator, do not change in size. This expansion appears to be a result of chain repulsion stretching the nylon fibers of the filter. This conclusion is supported by increases in expansion with both reaction time and with initiator density, and the fact that the filters do not return to their original size upon removal of solvent, although they do shrink to some extent. Re-wetting the filters swells them back to their swollen size before drying, and the extent of swelling is observed to be greater in solvents

known to be good solvents for PMMA. In addition, after the polymer is removed from the filters by cleavage, the filters return to approximately their original size.

Removal of the polymer chains from the nylon surface is accomplished by base hydrolysis, an approach similar to that employed in the past for bottle brush polymers.[29] The polymer from the brush is then analyzed and compared with polymer grown concurrently in solution. A notable difference between the solution grown and surface grown polymer is a low MW polymer fraction appearing in only the surface grown polymer. This low MW fraction remains in systems with added sacrificial initiator, although disparities in MW and PDI between solution and surface grown polymer are reduced. Figure 3 compares the GPC traces of polymer grown from sacrificial initiator in solution and polymer grown from initiator attached to the membrane surface, for a brush with 100 % initiator density after 23 hours of reaction time. The compared polymers are gown at the same time in the same reaction vessel. In all

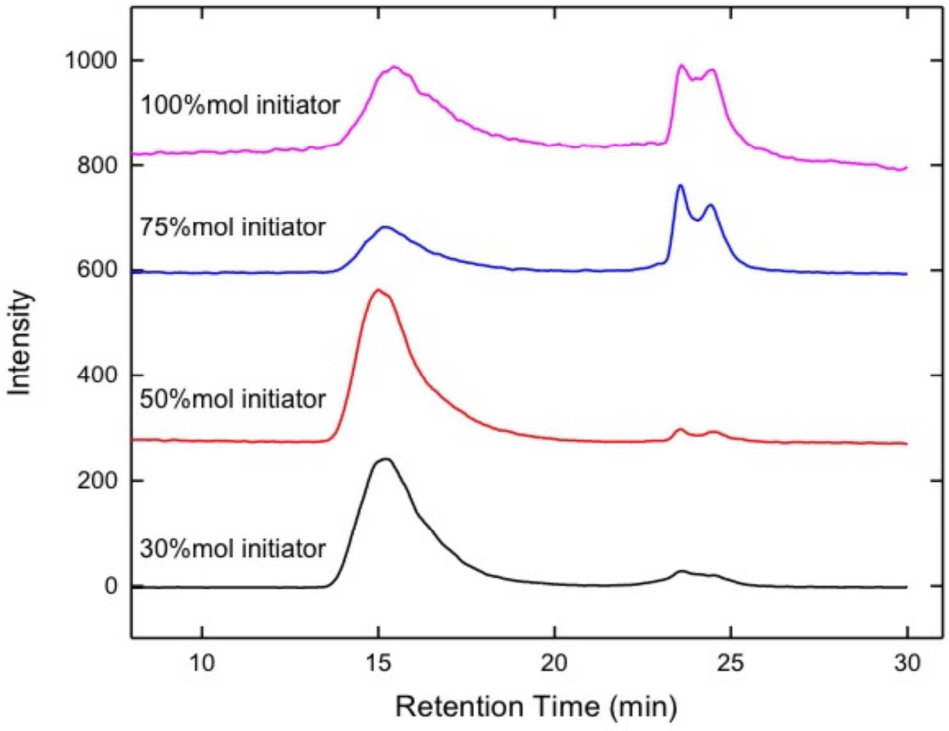

Figure 5. GPC spectra of polymers cleaved from nylon membranes made with varying molar ratios of BrIbB to IbB. Polymerizations were run for 11 hours. Increasing the density of initiator is shown to increase the fraction of low MW polymers grown from the surface.

cases we observe the MW to be higher and the PDI smaller for solution-grown polymer. This finding agrees with previous computational and experimental reports by Genzer[21,24], Milchev[25], and Kim[22].

The low MW material, however, is unexpected. To investigate the possibility it arises as a result of the conditions used to cleave chains from the membrane, either by low molecular weight nylon contaminants, hydrolysis, or degradation of PMMA, we compare the NMR spectra of polymer grown in solution with polymer cleaved from the surface, and find them to be identical (Figure 4). This verifies that the polymer is not hydrolyzed and that the nylon membrane did not degrade and contaminate the PMMA brush sample. This is especially compelling evidence as the low MW polymer fraction can constitute up to half the mass of the cleaved brush sample. If that mass were the result of degraded nylon filter or hydrolyzed PMMA, the NMR spectra of the solution grown and cleaved PMMA would be significantly different.

In order to show the low MW fraction is not the result of degrading the PMMA backbone, we compare the GPC traces of commercially obtained 35 Kg/mol PMMA before and after treatment with the conditions used to cleave chains from the membrane. The GPC shows the polymers to be unaffected (Figure SI4), thus the conditions used for cleaving the chains do not account for the low MW fraction. We are also reassured by the work of Sumita *et al*. studying the hydrolytic degradation of poly(L-lactide)/PMMA blends, who showed that, even with twice the hydroxide concentration as utilized in our cleaving step, only ploy(L-lactide) was degraded, leaving the PMMA unscathed.[30] Finally, to be sure the cleaved polymer is not simply solution grown polymer that had adsorbed to the surface of the nylon filter, extensive washing with THF is preformed prior to cleaving the attached polymer. The polymer collected prior to cleavage is also significantly different in MW from the polymer cut from the surface, arguing against it being the same material.

Although not affected by the addition of sacrifical initiator, the low MW polymer is affected by grafting density, as shown in Figure 5, and the mass and number fraction of the low MW polymer is shown in Table 1. The results are based on the low MW polymer having a MW of 2K. This number should be used with caution, however, as it is at the limit of the linear response of the GPC column. Ad-

ditionally, each ratio was run as a separate reaction, so small variations may be due to experimental variations and only larger trends are considered.

Table 1: Calculation of the ratios of high MW and low MW polymer fractions from GPC results.

Grafting ratio (ratio of initiator to blocker)	MW of high MW cleaved polymer (Kg/mole)	Mass fraction of low MW polymer	Number fraction of low MW polymer
100%	229	0.272	0.977
75 %	337	0.350	0.989
50 %	314	0.048	0.888
30 %	321	0.073	0.927

At low grafting densities, the amount of low MW polymer is barely discernable. The decrease in total mass of low MW chains with lower initiator density suggests that termination or monomer shielding is less prevalent when chains are less densely packed. This makes conceptual sense as radical chain ends that are more closely packed will have a greater probability of coupling and a more dense brush would be expected to impede monomer diffusion to a greater extent. Bimodal low MW peaks (Figure 5) are also observed with longer polymerizations runs, but not with shorter reaction times. It is tempting to explain this by chain coupling, but that would require that the growing polymers were starved of monomer more effectively by the higher MW polymers than is indicated by our simulations. Additionally, it is not clear if the MW of the low MW chains is affected by initiator density. While there appears to be a very slight increase in MW of the low MW fraction with decreasing grafting density, the decrease in retention time in the GPC is extremely small.

In order to see the effect of reaction time on the low MW brush material, we run a number of concurrent brush polymerizations and analyze them at various times. The result is shown in Figure 6. The 1-hour sample contains too little polymer for GPC analysis, however after two hours a significant low MW peak is seen along with a shoulder corresponding to growing brush chains. At the 2-hour point, the sample has a majority of chains that are short and a few that have grown to higher MW. As the polymerization time increases, the high molecular weight peak appears and increases in area relative to the low MW peak. It should be noted that the GPC indicates the mass of the polymer chains being analyzed, not the number of chains. Therefore the number of low MW chains remains very large in comparison to the higher MW chains. The number and mass fractions of the low MW polymer at 2, 4, and 8 eight hours is shown in the SI Table S2. The higher MW fraction increases with time due to the growth of chains that are neither terminated nor confined. The observation that mass increases more quickly early in the polymerization and more slowly after roughly two hours indicates that initially many chains are growing. As the number of either screened or terminated chains increases, fewer chains consume

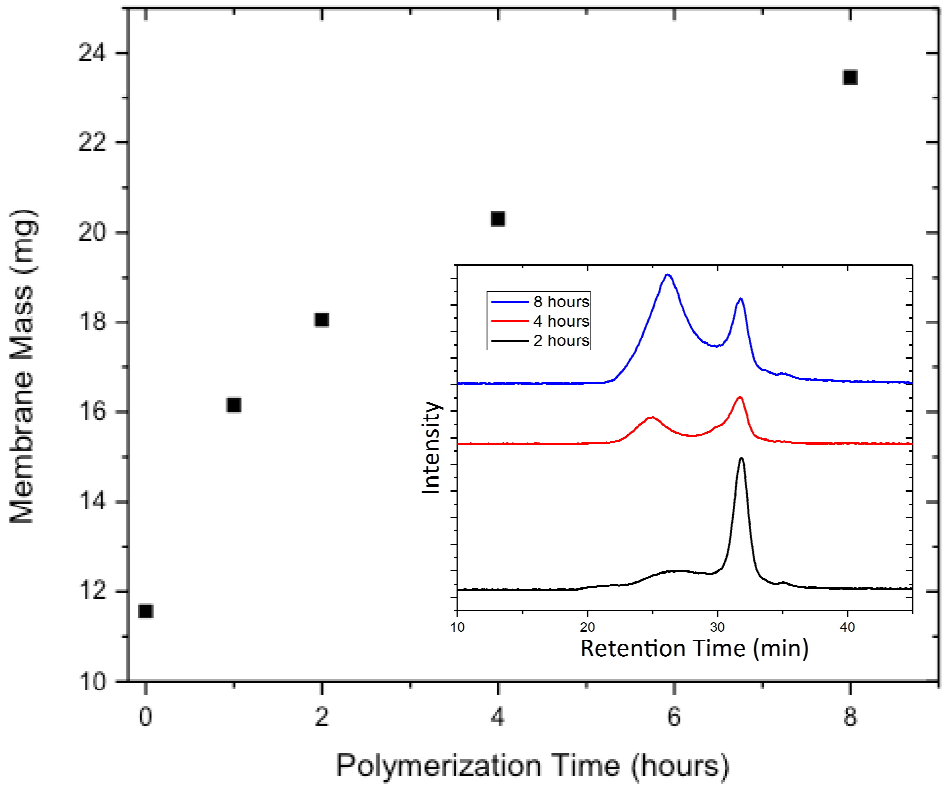

Figure 6. Mass of membranes as a function of polymerization time. Shown in the inset is the GPC of PMMA cleaved from filters after 2, 4, and 8 hours. The fraction of total polymer made up by low MW brushes decreases with reaction time.

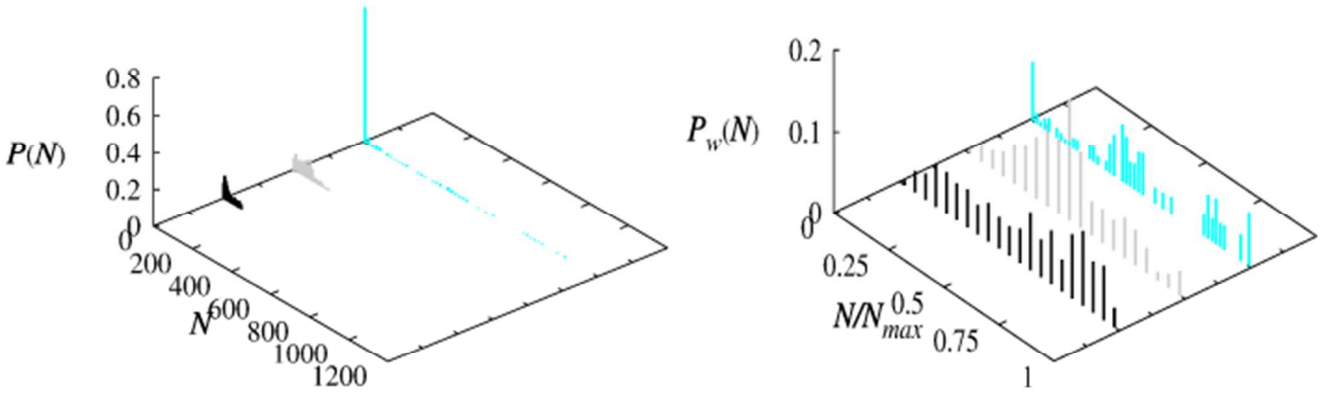

Figure 7. Number fraction, P(N), and weight fraction, $P_w(N)$, distribution functions of the chains in the growing brush layers obtained for two monomer conversions 22% (left) and 40% (right) as a function of the chain degree of polymerization N. Simulation results obtained for fast termination rate are shown by cyan bars, for slow termination rate are shown by gray bars and without termination are plotted as black bars.

monomer, and thus membrane mass increases more slowly.

In an effort to gain insight into the bimodal distribution of polymer chains grown from the filter surface, we perform molecular dynamics simulations of the brush polymerization at different surface initiator concentrations. We use a coarse-grained representation of monomers and polymer chains, where monomers are modeled by Lennard-Jones beads with diameter σ, and their connectivity in the polymer chains is maintained by the FENE potential. In our simulations to model a chain's recombination/termination, two growing chains combine with some probability by forming a bond if their active ends were within a capture radius from each other. Simulation details and the systems' set up are described in SI2. Our results for the evolution of the number fraction and weight fraction distribution function are as shown in Figure 7. This figure combines simulation data for the highest density of initiator on the substrate, ρ_g=0.385 σ^{-2}, and two different degrees of monomer conversion: 22% and 40%. The three sets of simulations presented in each graph in Figure 7 suggest the effect of chain termination by recombination on the distribution of chains the growing brush layer. In the simulations with fast recombination rate (equal to the propagation rate), shown in Figure 7 by cyan bars, we see a large peak in the number fraction distribution function, *P*(N), located at small values of chain degree of polymerization, N. This indicates the dominance of short loops in the number fraction distribution appearing with fast termination rates. With increasing time (conversion) the contribution of these chains to the weight frac-

tion distribution decreases as can be seen by comparing the weight fraction distribution functions for 22% and 40% conversion in Figure 7. Distribution functions are also obtained from two other simulations: one without termination (black bars) and one with a termination rate ten times slower than the polymerization rate (gray bars). For the slower termination rate, the number fraction distribution function $P(N)$ is very broad at conversion 22%, but at 40% conversion there is a peak corresponding to short chains. This is a manifestation of two effects: chain end termination and short chains being "screened" in the growing brush layer by the longer chains. (At high brush grafting density, the longer chains "starve" the shorter chains precluding available monomers from reaching the active chain ends of the short chains buried deep in the brush layer). This is confirmed by the change in the form of $P(N)$ for simulations without termination for which only the screening effect is possible. The weight fraction distribution functions are narrow, unlike the fast and slow termination simulations where we observe a growth in the center of the distribution function with increasing conversion. Although there are limitations to our simulation in terms of box size and ultimate degree of polymerization, the trend towards a multimodal distribution as a result of termination is apparent. At the DP's simulated in our system, the changing rate of propagation between the long and short chains has just started to become apparent.

CONCLUSIONS

Functionalizing high surface area substrates with varying initiator densities, polymer brushes are synthesized in quantities large enough to allow characterization of the bound brush polymers after removal from the surface, and simulations are preformed to better understand the results. GPC results indicate higher MW's and lower PDI's for solution grown chains compared to brush chains, and also reveals the presence of a low MW polymer fraction in all the brushes grown, with the mass ratio of low MW to high MW chains increasing with increasing initiator surface density. Longer reaction times (higher conversions) result in an increase in the mass of high MW chains relative to low MW chains, suggesting the continued growth of the longer chains and stagnation of the shorter ones. At very long reaction times (more than 100 hours) we observe a bimodal low MW peak suggestive of termination by radical recombination. These observations are explained in terms of a combination of termination and the screening of

monomer from shorter chains by longer chains. Initially the rate of propagation of all chains is nearly identical, but as the reaction progresses, the rate of polymerization for the longer and shorter chains diverges. This divergence in propagation rate due to shorter chains being starved of monomer increases as the degree of polymerization (DP) of growing chains increases, leading to increased dispersity of chain lengths in the final polymer brush. Molecular dynamics simulations, although somewhat limited in total DP, indicate that screening alone can not explain the bimodal or multimodal population and suggests the formation of a bimodal population of chain lengths with increasing DP is due largely to the chains' termination. Our results indicate that solution grown polymer gives an incomplete picture of surface grown chains, and suggests there may be an upper limit to the density of brushes possible by this widely used approach to polymer brush synthesis.

ASSOCIATED CONTENT

Supporting Information

The Supporting Information is available free of charge on the ACS Publications website at DOI:

AUTHOR INFORMATION

Corresponding Authors

*E-mail adobrynin@uakron.edu

*E-mail adamson@uconn.edu

ACKNOWLEDGEMENTS

This work was supported by the National Science Foundation under an AGEP GRS supplement to the Grant DMR-1004576 and NSF Grant CHE-1310453.

This research used resources of the Oak Ridge Leadership Computing Facility (OLCF), which is a DOE Office of Science User Facility supported under Contract DE-AC05-00OR22725.

REFERENCES

(1) Jeon, S. .; Lee, J. .; Andrade, J. .; De Gennes, P. . *J. Colloid Interface Sci.* **1991**, *142* (1), 149–158.

(2) Li, L.; Chen, S.; Zheng, J.; Ratner, B. D.; Jiang, S. *J. Phys. Chem. B* **2005**, *109* (7), 2934–2941.

(3) Rühe, J.; Yano, R.; Lee, J.-S.; Köberle, P.; Knoll, W.; Offenhäusser, A. *J. Biomater. Sci. Polym. Ed.* **1999**, *10* (8), 859–874.

(4) Hersel, U.; Dahmen, C.; Kessler, H. *Biomaterials* **2003**, *24* (24), 4385–4415.

(5) Sakata, H.; Kobayashi, M.; Otsuka, H.; Takahara, A. *Polym. J.* **2005**, *37* (10), 767–775.

(6) Kobayashi, M.; Terayama, Y.; Hosaka, N.; Kaido, M.; Suzuki, A.; Yamada, N.; Torikai, N.; Ishihara, K.; Takahara, A. *Soft Matter* **2007**, *3* (6), 740–746.

(7) Snaith, H. J.; Whiting, G. L.; Sun, B.; Greenham, N. C.; Huck, W. T. S.; Friend, R. H. *Nano Lett.* **2005**, *5* (9), 1653–1657.

(8) Paoprasert, P.; Spalenka, J. W.; Peterson, D. L.; Ruther, R. E.; Hamers, R. J.; Evans, P. G.; Gopalan, P. *J. Mater. Chem.* **2010**, *20* (13), 2651–2658.

(9) Maillard, D.; Kumar, S. K.; Rungta, A.; Benicewicz, B. C.; Prud'homme, R. E. *Nano Lett.* **2011**, *11* (11), 4569–4573.

(10) Ohno, K.; Ma, Y.; Huang, Y.; Mori, C.; Yahata, Y.; Tsujii, Y.; Maschmeyer, T.; Moraes, J.; Perrier, S. *Macromolecules* **2011**, *44* (22), 8944–8953.

(11) Lee, H.; Pietrasik, J.; Sheiko, S. S.; Matyjaszewski, K. *Prog. Polym. Sci.* **2010**, *35* (1-2), 24–44.

(12) Barbey, R.; Lavanant, L.; Paripovic, D.; Schüwer, N.; Sugnaux, C.; Tugulu, S.; Klok, H.-A. *Chem. Rev.* **2009**, *109* (11), 5437–5527.

(13) Milner, S. T. *Science* **1991**, *251* (February), 905–914.

(14) Klein, J.; Kumacheva, E.; Mahalu, D.; Perahla, D.; Fetters, L. J. *Nature* **1994**, *370*, 634–636.

(15) Zhao, B.; Brittain, W. J. *Macromolecules* **2000**, *33* (2), 342–348.

(16) Jordan, R.; Ulman, A.; Kang, J. F.; Rafailovich, M. H.; Sokolov, J. *J. Am. Chem. Soc.* **1999**, *121*, 1016–1022.

(17) Weck, M.; Jackiw, J. J.; Rossi, R. R.; Weiss, P. S.; Grubbs, R. H.; *J. Am. Chem. Soc.* **1999**, *121*, 4088–4089.

(18) Fujiki, K.; Sakamoto, M.; Yoshida, A.; Maruyama, H. *J. Polym. Sci. Part A Polym. Chem.* **1999**, *37* (13), 2121–2128.

(19) Azzaroni, O. *J. Polym. Sci. Part A Polym. Chem.* **2012**, *50* (16), 3225–3258.

(20) Marutani, E.; Yamamoto, S.; Ninjbadgar, T.; Tsujii, Y.; Fukuda, T.; Takano, M. *Polymer* **2004**, *45* (7), 2231–2235.

(21) Gorman, C. B.; Petrie, R. J.; Genzer, J., *Macromolecules* **2008**, *41*, 4856–4865.

(22) Kim, J.; Huang, W.; Miller, M. D.; Baker, G. L.; Bruening, M. L. *J. Polym. Sci. Part A Polym. Chem.* **2003**, *41*, 386–394.

(23) Patil, R. R.; Turgman-Cohen, S.; Šrogl, J.; Kiserow, D.; Genzer, J. *Langmuir* **2015**, *31* (8), 2372–2381.

(24) Turgman-Cohen, S.; Genzer, J. *J. Am. Chem. Soc.* **2011**, *133* (44), 17567–17569.

(25) Milchev, A.; Wittmer, J. P.; Landau, D. P. *J. Chem. Phys.* **2000**, *112* (3), 1606.

(26) Matyjaszewski, K.; Miller, P. J.; Shukla, N.; Immaraporn, B.; Gelman, A.; Luokala, B. B.; Siclovan, T. M.; Kickelbick, G.; Vallant, T.; Hoffmann, H.; Pakula, T. *Macromolecules* **1999**, *32*, 8716–8724.

(27) Huang, Wenxi; Kim, Jong-Bum; Bruening, Merlin L.; Baker, G. L. *Macromolecules* **2002**, *35*, 1175–1179.

(28) Xu, F. J.; Zhao, J. P.; Kang, E. T.; Neoh, K. G.; Li, J. *Langmuir* **2007**, *23* (16), 8585–8592.

(29) Sumerlin, B. S.; Neugebauer, D.; Matyjaszewski, K. *Macromolecules* **2005**, *38* (3), 702–708.

(30) Shirahase, T.; Komatsu, Y.; Tominaga, Y.; Asai, S.; Sumita, M. *Polymer* **2006**, *47* (13), 4839–4844.

TOC Image